Heliyon 7 (2021) e05893

Contents lists available at ScienceDirect

Heliyon

journal homepage: www.cell.com/heliyon

Research article

Synthesis, in silico ADME, molecular docking and in vitro cytotoxicity evaluation of stilbene linked 1,2,3-triazoles

Arnika Das [a,b,1], Sujeet Kumar [a,1], Leentje Persoons [c], Dirk Daelemans [c], Dominique Schols [c], Hakan Alici [d], Hakan Tahtaci [e], Subhas S. Karki [a,b,*]

[a] Department of Pharmaceutical Chemistry, KLE College of Pharmacy, Bengaluru, 560010, Karnataka, India
[b] Dr Prabhakar B Kore Basic Science Research Centre, Off-Campus, KLE College of Pharmacy, A Constituent Unit of KLE Academy of Higher Education and Research-Belagavi, Bengaluru, 560010, Karnataka, India
[c] Rega Institute for Medical Research, Department of Microbiology, Immunology and Transplantation, Laboratory of Virology and Chemotherapy, KU Leuven, B-3000, Leuven, Belgium
[d] Department of Physics, Faculty of Arts and Sciences, Zonguldak Bulent Ecevit University, 67100, Zonguldak, Turkey
[e] Department of Chemistry, Faculty of Science, Karabuk University, 78050, Karabuk, Turkey

ARTICLE INFO

Keywords:
Wittig reaction
1,2,3-Triazole
Cytotoxicity
ADME
Molecular docking

ABSTRACT

Series of (*E*)-1-benzyl-4-((4-styrylphenoxy)methyl)-1*H*-1,2,3-triazoles **7a-x** were obtained by Wittig reaction between 4-((1-benzyl-1*H*-1,2,3-triazol-4-yl)methoxy)benzaldehydes **5a-d** and benzyl triphenylphosphonium halides **6a-f** in benzene. The structures of the synthesized compounds were confirmed by FTIR, NMR (^{1}H and ^{13}C NMR) spectroscopy, and mass spectrometry. All synthesized compounds were screened for their cytotoxic activity against human cancer cell lines including pancreatic carcinoma, colorectal carcinoma, lung carcinoma, and leukemias such as acute lymphoblastic, chronic myeloid, and non-Hodgkinson lymphoma cell lines. *In vitro* cytotoxicity data showed that compounds **7c**, **7e**, **7h**, **7j**, **7k**, **7r**, and **7w** were moderately cytotoxic (11.6–19.3 μM) against the selected cancer cell lines. These cytotoxicity findings were supported using molecular docking studies of the compounds against 1TUB receptor. The drug-likeness properties of the compounds evaluated by *in silico* ADME analyses. Resveratrol linked 1,2,3-triazoles were more sensitive towards human carcinoma cell lines but least sensitive towards leukemia and lymphoma cell lines.

1. Introduction

Cancer is a group of diseases responsible for one in six deaths worldwide. To overcome this threat, effective methods such as immunotherapy, chemotherapy, surgery, and radiotherapy are needed. Each method has its advantages and disadvantages. Chemotherapeutic agents used to kill or inhibit the growth of cancer cells often have serious side effects, whereas radiotherapy and surgery are limited [1]. To fill this void, there is always a need for better alternatives. It is a daunting task to develop a new anticancer compound with improved pharmaceutical properties. The role of heterocyclic chemistry is commendable in this regard. Low toxicity, high regeneration, and better receptor binding make nitrogen (N) -containing heterocycle the first choice between synthons in the drug discovery process [2].

Three nitrogens and two carbon atoms of triazole contain a five heterocyclic compound ring, a 1,2,3-triazole ring exhibits a variety of biological functions, including antiviral, anti-inflammatory, antimicrobial and anti-tubercular. In addition, 1,4-disubstituted 1,2,3-triazoles show significant anticancer activity [3, 4, 5]. Recently Kaushik et al, developed and synthesized amide linked 1,4-disubstituted 1,2,3-triazoles (**I**) as an anticancer agents [6]. Murugavel et al, have been linked to the production of thiophen containing 1,2,3-triazole (**II**) and pyridine moiety as a potential for topoisomerase IIα inhibiting anticancer agents [7]. A series of connected chalcone 1,2,3 triazoles (**III**) was synthesized using a green chemical method and tested as anticancer agents [8].

Stilbene based compounds have attracted biologists and chemists because they are widely available in nature. They have a variety of biological functions [9, 10]. Hydroxylated stilbenes have been found in

* Corresponding author.
E-mail address: subhasskarki@gmail.com (S.S. Karki).
[1] Authors contributed equally.

https://doi.org/10.1016/j.heliyon.2020.e05893
Received 6 October 2020; Received in revised form 17 December 2020; Accepted 29 December 2020

medicinal plants but plain stilbene is not found in nature. *Trans*-3,5, 4′-trihydroxy stilbene (resveratrol) (**IV**) is found in grapes and plays a role in preventing coronary heart disease associated with the use of red wine [11, 12, 13]. This resveratrol exhibits the activity of many biological agents, such as chemopreventive [14] antioxidant [15] antineoplastic [16] and antiestrogenic [17]. Various extracts/structures of stilbenes show anticancer activity [18, 19, 20, 21].

In recent times, the molecular hybridization approach is a widely used techniques in drug discovery, which forms new molecular entities by incorporating stilbenes by linker through the methylene with 1,2,3-triazoles. These integrated or cohesive systems may have advanced biological properties related to specific substances. As the continuation of our work in small nitrogenous heterocyclic compounds, a series of E stilbene linked to 1,4-disubstituted-1,2,3-triazole derivatives (**7a-x**) were synthesized, identified, and in vitro cytotoxicity is performed in this paper (see Figure 1).

Furthermore, *in silico* ADME properties were investigated to determine the drug-likeness properties of the synthesized compounds using the SwissADME webserver [22, 23]. We also conducted docking simulations both to support the *in vitro* cytotoxicity studies of the compounds and to identify their binding sites on the 1TUB receptor (tubulin-docetaxel complex) [24].

2. Experimental

2.1. General information and instrumentation

Reagents and solvents were tested for purity before use. Melting points (m.p.) were measured by open capillary tube method in liquid paraffin (heavy) and are uncorrected. FTIR spectra were recorded using infrared (IR) grade potassium bromide (KBr) by diffuse reflectance technique on a JASCO 460 + instrument. The ^{1}H NMR spectra were recorded in deuterated dimethyl sulfoxide (DMSO-d_6) and chloroform ($CDCl_3$) in the range of 400–500 MHz (MHz) on Bruker (Ultraspec AMX 400) and JEOL RESONANCE instruments. Chemical shift (δ) values in ppm were expressed using tetramethylsilane (TMS) as the reference. Compound purity was determined by an Agilent 1100 HPLC coupled to an Agilent mass spectrometry detector (MSD) with electrospray ionization in positive mode. 4-(Prop-2-ynyloxy)benzaldehyde (**3**) and aryl azides (**4a-d**) were prepared as per literature [25] and 4-((1-arylmethyl-1*H*-1,2,3-triazol-4-yl)methoxy)benzaldehydes (**5a-d**) were synthesized as per the literature [26]. Various aryltriphenylphosphonium chlorides (**6a-f**) were prepared as per the literature [27].

2.2. Synthesis

General procedure for synthesis of (E)-1-benzyl-4-((4-styrylphenoxy)methyl)-1H-1,2,3-triazoles (7a-x)

Sodium hydride (0.0478 g, 2 mmol) was added in part to an equimolar mixture of different benzyltriphenylphosphonium halides (**6a-f**) and 4-((1-benzyl-1*H*-1,2,3-triazol-4-yl)methoxy) benzaldehydes **(5a-d)** at 0–5 °C in dry benzene. The resulting mixture was stirred for 16 h at room temperature. Excess sodium hydride was quenched in anhydrous methanol (10 mL) followed by extraction with a chloroform-water mixture. The organic layer was dried over anhydrous Na_2SO_4 and removed under vacuum. The crude mass thus obtained was purified from hot ethanol to get the ***E*** isomeric forms of **7a-x** while ***Z*** remained in the solution.

(E)-1-benzyl-4-((4-styrylphenoxy) methyl)-1H-1,2,3-triazole (7a). White amorphous mass, IR (KBr) *ν*: = 3010, 2873, 1602, 1510, 1455, 1243 cm^{-1}. ^{1}H NMR (400 MHz, DMSO-d_6): δ = 5.15 (2H, s, –CH_2-), 5.61 (2H, s, –OCH_2-), 7.04 (2H, d, J = 8.8 Hz, Ar–H), 7.11 (1H, d, *J* = 16.4 Hz, styryl –CH=C-), 7.17–7.25 (2H, md, *J* = 16.4 Hz, styryl –C=CH-), 7.30–7.39 (7H, m, Ar–H), 7.54 (4H, m, Ar–H), 8.27 (1H, s, Triazole-H). ^{13}C NMR (400 MHz, DMSO-d_6): δ = 52.82, 61.12, 114.97, 124.66, 126.16, 126.30, 127.06, 127.19, 127.75, 127.93, 128.13, 128.63, 128.74, 157.72. +MS (ESI) m/z: 369.1 (368.4).

(E)-1-benzyl-4-((4-(4-fluorostyryl)-phenoxy)methyl)-1H-1,2,3-triazole (7b). White amorphous mass, IR (KBr) *ν*: = 3074, 2790, 1605, 1514, 1455, 1266 cm-^{1}. ^{1}H NMR (400 MHz, DMSO-d_6): δ = 5.15 (2H, s, –CH_2-), 5.60 (2H, s, –OCH_2-), 7.04 (2H, d, *J* = 11.6 Hz, Ar–H), 7.12 (2H, d, *J* = 6.8 Hz, Ar–H), 7.16–7.20 (2H, m, Ar–H), 7.30–7.39 (5H, m, Ar–H), 7.53 (2H, d, *J* = 11.2 Hz, Ar–H), 7.58–7.61 (2H, m, Ar–H), 8.27 (1H, s, Triazole-H). ^{13}C NMR (400 MHz, DMSO-d_6): δ = 52.84, 61.11, 114.97, 115.43, 115.60, 124.72, 125.15, 127.73, 127.91, 127.96, 128.01, 128.17, 128.78, 129.95, 133.97, 136.02, 142.94, 157.73, 160.43, 162.37. +MS (ESI) m/z: 386.1 (386.4).

(E)-1-benzyl-4-((4-(4-chlorostyryl)phenoxy)methyl)-1H-1,2,3-triazole (7c). White crystals, IR (KBr) *ν*: = 3033, 2918, 1603, 1509, 1467, 1249 cm-^{1}. ^{1}H NMR (400 MHz, DMSO-d_6): δ = 5.15 (2H, s, –CH_2-), 5.60 (2H, s, –OCH_2-), 7.03 (2H, d, *J* = 8.4 Hz, Ar–H), 7.11 (1H, d, J = 16.8 Hz, styryl –CH=C-), 7.23 (1H, d, *J* = 16.8 Hz, styryl –C=CH-),

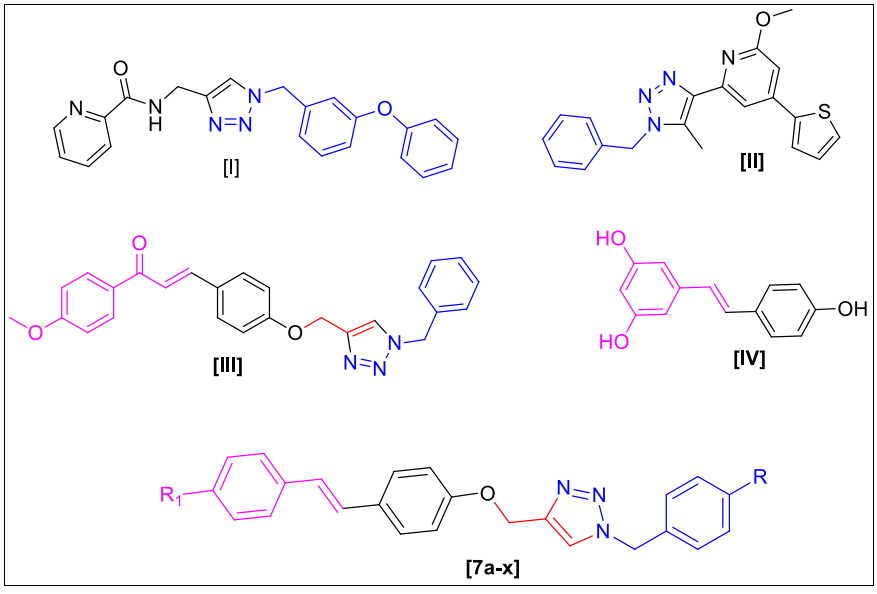

Figure 1. Pharmacologically hybridized/linked 1,2,3-triazole derivatives such as amide linked 1,4-disubstituted 1,2,3-triazoles I, thiophen containing 1,2,3-triazole pyridine II, chalcone linked 1,2,3-triazole III, resveratrol IV and resveratrol linked 1,2,3-triazoles 7a-x.

7.29–7.38 (3H, m, Ar–H), 7.45 (2H, d, $J = 8.8$ Hz, Ar–H), 7.55 (2H, d, $J = 8.8$ Hz, Ar–H), 7.54 (2H, d, $J = 8.8$ Hz, Ar–H), 8.27 (1H, s, Triazole-H). ^{13}C NMR (400 MHz, DMSO-d_6): δ = 53.37, 61.66, 115.53, 125.25, 125.51, 128.35, 128.44, 128.49, 128.70, 129.17, 129.31, 129.42, 130.30, 131.94, 136.55, 136.90, 139.73, 143.44, 158.43. +MS (ESI) m/z: 402.1 (402.9).

(E)-1-benzyl-4-((4-(4-methylstyryl)phenoxy)methyl)-1H-1,2,3-triazole (7d). White crystals, IR (KBr) ν: = 3070, 2964, 1603, 1514, 1476, 1244 cm-^{1}. ^{1}H NMR (400 MHz, DMSO-d_6): δ = 2.29 (3H, s, –CH_3), 5.14 (2H, s, –CH_2-), 5.60 (2H, s, 2H, –OCH_2-), 7.03 (2H, d, $J = 8.8$ Hz, Ar–H), 7.06 (1H, d, $J = 16.8$ Hz, styryl –CH=C-), 7.10 (1H, d, $J = 16.8$ Hz, styryl –C=CH-), 7.17 (2H, d, $J = 8$ Hz, Ar–H), 7.29–7.39 (4H, m, Ar–H), 7.45 (2H, d, $J = 8$ Hz, Ar–H), 7.52 (2H, d, $J = 8.8$ Hz, Ar–H), 8.27 (1H, s, Triazole-H). ^{13}C NMR (400 MHz, DMSO-d_6): = δ 20.78, 52.81, 61.10, 124.65, 126.08, 126.23, 126.39, 127.57, 127.92, 128.12, 128.73, 129.23, 130.13, 134.53, 135.98, 136.50, 143.05, 157.59, 178.69. +MS (ESI) m/z: 382.1 (382.5).

(E)-1-benzyl-4-((4-(4-methoxystyryl)phenoxy)methyl)-1H-1,2,3-triazole (7e). White amorphous mass, IR (KBr) ν: = 3034, 2837, 1606, 1514, 1467, 1384, 1253 cm-^{1}. ^{1}H NMR (400 MHz, DMSO-d_6): δ = 3.76 (3H, s, –OCH_3), 5.14 (2H, s, –CH_2-), 5.60 (2H, s, –OCH_2-), 6.93 (2H, d, $J = 8.8$ Hz, Ar–H), 6.99–7.03 (4H, m, Ar–H), 7.30–7.39 (5H, m, Ar–H), 7.49 (4H, d, $J = 8$ Hz, Ar–H), 8.27 (1H, s, Triazole-H). ^{13}C NMR (400 MHz, DMSO-d_6): δ = 52.82, 55.11, 61.11, 114.11, 114.93, 124.65, 125.69, 125.95, 127.37, 127.42, 127.93, 128.13, 128.74, 129.97, 130.36, 135.99, 142.96, 157.38, 158.65. +MS (ESI) m/z: 398.1 (398.5).

(E)-1-benzyl-4-((4-(4-nitrostyryl) phenoxy)methyl)-1H-1,2,3-triazole (7f). Yellow crystals, IR (KBr) ν: = 3101, 2838, 1591, 1513, 1178 cm-^{1}. ^{1}H NMR (400 MHz, DMSO-d_6): δ = 5.18 (2H, s, –CH_2-), 5.61 (2H, s, –OCH_2-), 7.09 (2H, d, $J = 8.8$ Hz, Ar–H), 7.29 (1H, d, $J = 16.4$ Hz, styryl –CH=C-), 7.30–7.39 (5H, m, Ar–H), 7.50 (1H, d, $J = 16.4$ Hz, styryl –C=CH-), 7.63 (2H, d, $J = 8.8$ Hz, Ar–H), 7.82 (2H, d, $J = 8.8$ Hz, Ar–H), 8.22 (2H, d, $J = 8.8$ Hz, Ar–H), 8.28 (1H, s, Triazole-H). ^{13}C NMR (400 MHz, DMSO-d_6): δ = 53.40, 61.70, 115.65, 124.61, 124.75, 125.32, 127.47, 128.52, 128.73, 129.18, 129.33, 129.81, 133.52, 136.56, 143.37, 145.04, 146.37, 159.13. +MS (ESI) m/z: 413.1 (413.4).

(E)-1-(4-nitrobenzyl)-4-((4-styrylphenoxy)methyl)-1H-1,2,3-triazole (7g). Yellow amorphous powder, IR (KBr) ν: = 3087, 2872, 1606, 1515, 1447, 1219 cm-^{1}. ^{1}H NMR (400 MHz, DMSO-d_6): δ = 5.18 (2H, s, –CH_2-), 5.80 (2H, s,–OCH_2–), 7.05 (2H, d, $J = 8.8$ Hz, Ar–H), 7.11 (1H, d, $J = 16.4$ Hz, styryl –CH=C-), 7.21 (1H, d, $J = 16.8$ Hz, styryl –C=CH-), 7.25 (1H, d, $J = 7.2$ Hz, Ar–H), 7.35 (2H, t, $J = 15.6$ Hz, Ar–H), 7.51–7.56 (5H, m, Ar–H), 8.25 (2H, d, $J = 8.0$ Hz, Ar–H), 8.38 (1H, s, Triazole-H). ^{13}C NMR (400 MHz, DMSO-d_6): δ = 51.92, 61.10, 114.99, 123.95, 125.16, 126.19, 126.34, 127.23, 127.79, 127.95, 128.67, 129.05, 130.05, 137.33, 143.12, 143.42, 147.25, 157.69. +MS (ESI) m/z: 414.1 (413.4).

(E)-4-((4-(4-fluorostyryl)phenoxy)methyl)-1-(4-nitrobenzyl)-1H-1,2,3-triazole (7h). Light yellow crystals, IR (KBr) ν: = 3098, 2874, 1607, 1517, 1458, 1217 cm-^{1}. ^{1}H NMR (400 MHz, DMSO-d_6): δ 5.18 (2H, s, –CH_2-), 5.80 (2H, s, –OCH_2-), 7.05 (d, 2H, $J = 9.2$, Hz Ar–H), 7.12 (2H, d, $J = 6.4$ Hz, Ar–H), 7.16–7.20 (2H, m, Ar–H), 7.51–7.54 (4H, m, Ar–H), 7.57–7.61 (2H, m, Ar–H), 8.24 (2H, d, $J = 8.8$ Hz, Ar–H), 8.35 (1H, s, Triazole-H). ^{13}C NMR (400 MHz, DMSO-d_6): δ = 51.92, 61.11, 115.00, 115.19, 115.39, 115.56, 123.90, 125.10, 125.17, 127.71, 127.87, 127.92, 127.99, 129.01, 129.98, 131.75, 133.91, 143.12, 143.36, 147.24, 157.67, 160.41, 162.35. +MS (ESI) m/z: 431.1 (431.4).

(E)-4-((4-(4-chlorostyryl)phenoxy)methyl)-1-(4-nitrobenzyl)-1H-1,2,3-triazole (7i). Yellow amorphous mass, IR (KBr) ν: = 3084, 2781, 1604, 1514, 1457, 1348, 1256 cm-^{1}. ^{1}H NMR (400 MHz, DMSO-d_6): δ = 5.18 (2H, s, –CH_2-), 5.80 (2H, s, –OCH_2-), 7.05 (2H, d, $J = 8.8$ Hz, Ar–H), 7.11 (1H, d, $J = 16.8$ Hz, styryl –CH=C-), 7.24 (1H, d, $J = 16.8$ Hz, styryl –C=CH-), 7.41 (2H, d, $J = 8.8$ Hz, Ar–H), 7.51–7.55 (4H, m, Ar–H), 7.58 (2H, d, $J = 8.4$ Hz, Ar–H), 8.24 (2H, d, $J = 8.8$ Hz, Ar–H), 8.35 (1H, s, Triazole-H).^{13}C NMR (400 MHz, DMSO-d_6): δ = 51.94, 61.11, 115.04, 123.96, 125.01, 125.18, 127.83, 127.94, 128.65, 128.87, 129.06, 129.82, 131.44, 136.37, 143.11, 143.42. +MS (ESI) m/z: 448.0 (447.9).

(E)-4-((4-(4-methylstyryl)phenoxy)methyl)-1-(4-nitrobenzyl)-1H-1,2,3-triazole (7j). Yellow crystals, IR (KBr) ν: = 3087, 2912, 1604, 1515, 1453, 1349, 1255 cm^{-1}. ^{1}H NMR (400 MHz, DMSO-d_6): δ = 2.29 (3H, s, –CH_3), 5.17 (2H, s, –CH_2-), 5.80 (2H, s, –OCH_2-), 7.04 (2H, d, $J = 8.8$ Hz, Ar–H), 7.06 (1H, s, $J = 16$ Hz, styryl –CH=C-), 7.10 (1H, s, $J = 16$ Hz, styryl –C=CH-), 7.17 (2H, d, $J = 8.0$ Hz, Ar–H), 7.45 (2H, d, $J = 8.0$ Hz, Ar–H), 7.50–7.54 (4H, dd, Ar–H), 8.24 (2H, d, $J = 8.8$ Hz, Ar–H), 8.35 (1H, s, Triazole-H). ^{13}C NMR (400 MHz, DMSO-d_6): δ = 20.80, 51.91, 61.08, 114.97, 123.92, 125.13, 126.27, 126.92, 127.61, 129.03, 129.25, 130.19, 134.53, 136.53, 143.13, 143.39, 147.24, 157.52. +MS (ESI) m/z: 427.1 (427.5).

(E)-4-((4-(4-methoxystyryl)phenoxy)methyl)-1-(4-nitrobenzyl)-1H-1,2,3-triazole (7k). Yellow amorphous mass, IR (KBr) ν: = 3087, 2836, 1607, 1516, 1462, 1349, 1254 cm^{-1}. ^{1}H NMR (400 MHz, DMSO-d_6): δ = 3.76 (3H, s, –OCH_3), 5.17 (2H, s, –CH_2-), 5.79 (2H, s, –OCH_2-), 6.93 (2H, d, $J = 8$ Hz, Ar–H), 7.00–7.03 (4H, m, Ar–H), 7.49 (4H, d, $J = .$ 8.4 Hz, Ar–H), 7.53 (2H, d, $J = 9$ Hz, Ar–H), 8.24 (2H, d, $J = 8.8$ Hz, Ar–H), 8.34 (1H, s, Triazole-H).^{13}C NMR (400 MHz, DMSO-d_6): δ = 51.91, 55.11, 61.08, 114.11, 114.96, 123.92, 125.11, 125.07, 126.02, 127.43, 129.03, 129.96, 130.41, 143,15, 143.39, 147.24, 157.34, 158.65. +MS (ESI) m/z: 444.1 (443.5).

(E)-1-(4-nitrobenzyl)-4-((4-(4-nitrostyryl)phenoxy)methyl)-1H-1,2,3-triazole (7l). Yellow amorphous mass, IR (KBr) ν: = 3050, 2936, 1588, 1507, 1176 cm^{-1}. ^{1}H NMR (400 MHz, DMSO-d_6): δ = 5.20 (2H, s, –CH_2-), 5.80 (2H, s, –OCH_2-), 7.09 (2H, d, $J = 8.8$ Hz, Ar–H), 7.29 (1H, d, $J = 16.4$ Hz, styryl –CH=C-), 7.50 (1H, d, $J = 16.4$ Hz, styryl –C=CH-), 7.54 (2H, d, $J = 8.4$ Hz, Ar–H), 7.63 (2H, d, $J = 8.8$ Hz, Ar–H), 7.82 (2H, d, $J = 8.8$ Hz, Ar–H), 8.22 (2H, d, $J = 9.2$ Hz, Ar–H), 8.25 (2H, d, $J = 8.8$ Hz, Ar–H), 8.36 (1H, s, Triazole-H).^{13}C NMR (400 MHz, DMSO-d_6): δ = 51.93, 61.14, 115.13, 123.92, 124.03, 124.23, 125.16, 126.90, 128.62, 129.04, 129.29, 132.93, 143.00, 143.37, 144.46, 145.82, 158.52. +MS (ESI) m/z: 458.0 (458.4).

(E)-1-(4-methylbenzyl)-4-((4-styrylphenoxy) methyl)-1H-1,2,3-triazole (7m). White crystals, IR (KBr) ν: = 3027, 2872, 1602, 1509, 1462, 1380, 1243 cm^{-1}. ^{1}H NMR (400 MHz, DMSO-d_6): δ = 2.27 (3H, s, –CH_3), 5.14 (2H, s, –CH_2-), 5.54 (2H, s, –OCH_2-), 7.04 (2H, d, $J = 8.8$ Hz, Ar–H), 7.07 (1H, d, $J = 16.4$ Hz, styryl –CH=C-), 7.16–7.25 (6H, m, Ar–H), 7.35 (2H, t, $J = 16.0$ Hz, Ar–H), 7.55 (4H, t, $J = 16.8$ Hz, Ar–H), 8.23 (1H, s, Triazole-H).^{13}C NMR (400 MHz, DMSO-d_6): δ 20.67, 52.63, 61.11, 114.96, 124.54, 126.16, 126.29, 127.20, 127.76, 127.99, 128.65, 129.28, 129.98, 132.99, 137.33, 137.49, 142.88, 157.72. +MS (ESI) m/z: 382.0 (382.5).

(E)-4-((4-(4-fluorostyryl)phenoxy)methyl)-1-(4-methylbenzyl)-1H-1,2,3-triazole (7n). White amorphous powder, IR (KBr) ν: = 3077, 2872, 1605, 1514, 1454, 1213 cm-^{1}. NMR (400 MHz, DMSO-d_6): δ = 2.27 (3H, s, –OCH_3), 5.14 (2H, s, –CH_2-), 5.54 (2H, s, –OCH_2-), 7.04 (2H, d, $J = 8.8$ Hz, Ar–H), 7.12 (2H, d, $J = 6.8$ Hz, Ar–H), 7.16–7.22 (6H, m, Ar–H), 7.52 (2H, d, $J = 8.4$ Hz, Ar–H), 7.57–7.61 (2H, m, Ar–H), 8.23 (1H, s, Triazole-H). ^{13}C NMR (400 MHz, DMSO-d_6): δ 20.63, 52.60, 61.10, 114.95, 115.34, 115.55, 124.47, 125.11, 127.67, 127.88, 127.95, 129.24, 129.91, 132.95, 133.93, 137.45, 142.85, 157.68. +MS (ESI) m/z: 400.1 (400.5).

(E)-4-((4-(4-chlorostyryl)phenoxy) methyl)-1-(4-methylbenzyl)-1H-1,2,3-triazole (7o). White amorphous mass, IR (KBr) ν: = 3077, 2877, 1605, 1510, 1457, 1177 cm^{-1}. ^{1}H NMR (400 MHz, DMSO-d_6): δ = 2.27 (3H, s, –CH_3), 5.14 (2H, s, –CH_2-), 5.54 (2H, s, –OCH_2-), 7.04 (2H, d, $J = 8.8$ Hz, Ar–H), 7.11 (1H, d, $J = 16.4$ Hz, styryl –CH=C-), 7.16–7.23 (5H, m, Ar–H), 7.40 (2H, d, $J = 8.8$ Hz, Ar–H), 7.54 (2H, d, $J = 8.8$ Hz, Ar–H), 7.59 (2H, d, $J = 8.8$ Hz, Ar–H), 8.23 (1H, s, Triazole-H). ^{13}C NMR (400 MHz, DMSO-d_6): δ = 20.67, 52.62, 61.09, 114.95, 115.41, 115.58, 124.54, 125.13, 127.70, 127.93, 127.99, 129.28, 129.92, 132.99, 133.93, 137.50, 142.87, 157.70, 160.41, 162.32. +MS (ESI) m/z: 416.1 (416.9).

(E)-1-(4-methylbenzyl)-4-((4-(4-methylstyryl)phenoxy)methyl)-1H-1,2,3-triazole (7p). White crystals, IR (KBr) ν: = 3023, 2734, 1602, 1515, 1455, 1388, 1240 cm^{-1}. ^1H NMR (400 MHz, DMSO-d_6): δ = 2.27 (3H, s, $–CH_3$), 2.29 (3H, s, $–CH_3$-), 5.13 (2H, s, $–CH_2$-), 5.40 (2H, s,$–OCH_2–$), 7.02 (2H, d, J = 8.8 Hz, Ar–H), 7.06 (1H, s, J = 16.8 Hz, styryl –CH=C-), 7.10 (1H, s, J = 16.8 Hz, styryl –C=CH-), 7.15–7.22 (6H, m, Ar–H), 7.45 (2H, d, J = 8.0 Hz, Ar–H), 7.51 (2H, d, J = 8.8 Hz, Ar–H), 8.23 (1H, s, Triazole-H). ^{13}C NMR (400 MHz, DMSO-d_6): δ 20.65, 20.78, 52.61, 61.1.0, 113.70, 114.94, 124.49, 126.08, 126.22, 126.93, 127.57, 127.97, 129.22, 129.26, 130.25, 133.01, 134.50, 136.49, 137.59, 142.89, 157.55. +MS (ESI) m/z: 396.1 (396.5).

(E)-4-((4-(4-methoxystyryl)phenoxy)methyl)-1-(4-methylbenzyl)-1H-1,2,3-triazole (7q). White amorphous mass, IR (KBr) ν: = 3079, 2840, 1605, 1515, 1395, 1249 cm^{-1}. ^1H NMR (400 MHz, DMSO-d_6): δ = 2.27 (3H, s, $–CH_3$), 3.76 (3H, s, 3H, $–OCH_3$), 5.13 (2H, s, $–CH_2$-), 5.54 (2H, s, $–OCH_2$-), 6.93 (2H, d, J = 8.8 Hz, Ar–H), 6.99–7.02 (4H, m, Ar–H), 7.16–7.22 (4H, m, Ar–H), 7.47–7.50 (4H, m, Ar–H), 8.23 (1H, s, Triazole-H). ^{13}C NMR (400 MHz, DMSO-d_6): δ = 20.66, 52.62, 55.11, 61.10, 114.11, 114.93, 124.49, 125.69, 125.98, 127.37, 127.41, 127.97, 129.27, 129.97, 130.35, 132.99, 137.48, 142.92, 157.37, 158.64. +MS (ESI) m/z: 412.1 (412.5).

(E)-1-(4-methylbenzyl)-4-((4-(4-nitrostyryl)phenoxy)methyl)-1H-1,2,3-triazole (7r). White crystals, IR (KBr) ν: = 3075, 2926, 1592, 1509, 1465, 1388, 1219 cm^{-1}. ^1H NMR (400 MHz, DMSO-d_6): δ = 2.27 (3H, s, $–CH_3$), 5.17 (2H, s, $–CH_2$-), 5.54 (2H, s, $–OCH_2$-), 7.08 (2H, d, J = 8.4 Hz, Ar–H), 7.18 (2H, d, J = 8 Hz, Ar–H), 7.22 (2H, d, J = 8 Hz, Ar–H), 7.29 (1H, d, J = 16.4 Hz, styryl –CH=C-), 7.50 (1H, d, J = 16.4 styryl –C=CH-), 7.63 (2H, d, J = 8.8 Hz, Ar–H), 7.82 (2H, d, J = 9.2 Hz, Ar–H), 8.22 (2H, d, J = 8.8 Hz, Ar–H), 8.24 (1H, s, Triazole-H). ^{13}C NMR (400 MHz, DMSO-d_6): δ = 20.67, 52.64, 61.13, 115.09, 124.03, 124.18, 124.58, 126.89, 127.99, 128.61, 129.29, 132.96, 137.51, 142.76, 144.47, 145.81, 158.56. +MS (ESI) m/z: 427.1 (427.5).

(E)-1-(4-chlorobenzyl)-4-((4-styrylphenoxy)methyl)-1H-1,2,3-triazole (7s). White crystals, IR (KBr) ν: = 3023, 2791, 1606, 1516, 1459, 1258 cm^{-1}. ^1H NMR (400 MHz, DMSO-d_6): δ = 5.15 (2H, s, $–CH_2$-), 5.61 (2H, s, $–OCH_2$-), 7.04 (2H, d, J = 8.8 Hz, Ar–H), 7.11 (1H, d, J = 16.4 Hz, styryl –CH=C-), 7.21 (1H, d, J = 16.4 Hz, styryl –C=CH-), 7.25 (1H, d, J = 7.2 Hz, Ar–H), 7.32–7.37 (4H, m, Ar–H), 7.45 (2H, d, J = 8.4 Hz, Ar–H), 7.56 (4H, t, J = 15.2 Hz, Ar–H), 8.28 (1H, s, Triazole-H). ^{13}C NMR (400 MHz, DMSO-d_6): δ = 51.01, 61.11, 114.97, 115.19, 124.73, 126.16, 126.31, 127.19, 127.76, 127.95, 128.63, 128.75, 129.89, 130.01, 131.75, 132.87, 134.98, 137.32, 142.99, 157.70, 191.38. +MS (ESI) m/z: 402.1 (402.9).

(E)-1-(4-chlorobenzyl)-4-((4-(4-fluorostyryl)phenoxy)methyl)-1H-1,2,3-triazole (7t). White crystals, IR (KBr) ν: = 3064, 2790, 1607, 1515, 1459, 1216 cm^{-1}. ^1H NMR (400 MHz, DMSO-d_6): δ 5.15 = (3H, s, $–CH_2$), 5.61 (2H, s, $–OCH_2$-), 7.04 (2H, d, J = 8.8 Hz, Ar–H), 7.12 (2H, d, J = 6.4 Hz, Ar–H), 7.16–7.20 (2H, m, Ar–H), 7.34 (2H, d, J = 10.8 Hz, Ar–H), 7.45 (2H, d, J = 8.4 Hz, Ar–H), 7.53 (2H, d, J = 11.6 Hz, Ar–H), 7.58–7.61 (2H, m, Ar–H), 8.28 (1H, s, Triazole-H). ^{13}C NMR (400 MHz, DMSO-d_6): = δ 52.0, 61.10, 114.97, 115.40, 115.57, 124.73, 125.15, 127.70, 127.88, 127.92, 127.99, 128.75, 129.89, 129.95, 132.86, 133.92, 134.98, 142.98, 157.69, 160.41, 162.34. +MS (ESI) m/z: 420.0 (420.9).

(E)-1-(4-chlorobenzyl)-4-((4-(4-chlorostyryl)phenoxy)methyl)-1H-1,2,3-triazole (7u). White crystals, IR (KBr) ν: = 3059, 2937, 1606, 1514, 1492, 1258 cm^{-1}. ^1H NMR (400 MHz, DMSO-d_6): δ = 5.15 (2H, s, $–CH_2$-), 5.61 (2H, s, $–OCH_2$-), 7.05 (2H, d, J = 8.8 Hz, Ar–H), 7.11 (1H, d, J = 16.8 Hz, styryl –CH=C-), 7.24 (1H, d, J = 16.8 Hz, styryl –C=CH-), 7.34 (2H, d, J = 8.4 Hz, Ar–H), 7.38–7.46 (4H, dd, J = 8.8, 8.8 Hz, Ar–H), 7.52–7.59 (4H, dd, J = 8.4, 8.8 Hz, Ar–H), 8.20 (1H, s, Triazole-H). ^{13}C NMR (400 MHz, DMSO-d_6): δ = 52.01, 61.11, 124.74, 124.97, 127.78, 127.88, 128.61, 128.75, 128.86, 129.77, 129.89, 131.39, 132.86, 134.98, 136.34, 142.95, 157.86. +MS (ESI) m/z: 437.0 (437.3).

(E)-1-(4-chlorobenzyl)-4-((4-(4-methylstyryl)phenoxy)methyl)-1H-1,2,3-triazole (7v). White crystals, IR (KBr) ν: = 3087, 2921, 1604, 1514, 1459, 1336, 1253 cm^{-1}. ^1H NMR (400 MHz, DMSO-d_6): δ = 2.29 (3H, s, $–CH_3$), 5.15 (2H, s, $–CH_2$-), 5.61 (2H, s, $–OCH_2$-), 7.02 (2H, d, J = 8.8 Hz, Ar–H), 7.06 (1H, d, J = 16 Hz, styryl –CH=C-), 7.10 (1H, d, J = 16 Hz, styryl –C=CH-), 7.17 (2H, d, J = 7.6 Hz, Ar–H), 7.36 (2H, d, J = 8.4 Hz, Ar–H), 7.45 (4H, d, J = 8.4 Hz, Ar–H), 7.51 (2H, d, J = 8.8 Hz, Ar–H), 8.27 (1H, s, Triazole-H). ^{13}C NMR (400 MHz, DMSO-d_6): δ = 20.78, 51.99, 61.10, 114.95, 124.71, 126.09, 126.25, 126.93, 127.85, 128.74, 129.23, 129.88, 130.16, 132.85, 134.53, 134.97, 136.51, 143.0, 157.54. +MS (ESI) m/z: 416.1 (416.9).

(E)-1-(4-chlorobenzyl)-4-((4-(4-methoxystyryl)phenoxy)methyl)-1H-1,2,3-triazole (7w). White amorphous mass, IR (KBr) ν: = 3077, 2841, 1606, 1516, 1388, 1251 cm^{-1}. ^1H NMR (400 MHz, DMSO-d_6): δ = 3.76 (3H, s, $–OCH_3$), 5.14 (2H, s, $–CH_2$-), 5.61 (2H, s, $–OCH_2$-), 6.93 (2H, d, J = 8.8 Hz, Ar–H), 7.00–7.03 (4H, m, Ar–H), 7.34 (2H, d, J = 8.4 Hz, Ar–H), 7.45 (2H, d, J = 8.4 Hz, Ar–H), 7.50 (4H, d, J = 8.8 Hz, Ar–H), 8.28 (1H, s, Triazole-H). ^{13}C NMR (400 MHz, DMSO-d_6): δ = 51.99, 55.10, 61.10, 114.10, 114.94, 124.68, 125.68, 125.99, 127.36, 128.74, 129.88, 129.96, 130.37, 132.85, 134.97, 143.02, 157.35, 158.64. +MS (ESI) m/z: 432.1 (432.9).

(E)-1-(4-chlorobenzyl)-4-((4-(4-nitrostyryl)phenoxy)methyl)-1H-1,2,3-triazole (7x). Yellow crystals, IR (KBr) ν: = 3089, 2826, 1634, 1587, 1509, 1427, 1217 cm^{-1}. ^1H NMR (400 MHz, DMSO-d_6): δ = 5.18 (2H, s, $–CH_2$-), 5.62 (2H, s, $–OCH_2$-), 7.09 (2H, d, J = 8.8 Hz, Ar–H), 7.29 (1H, d, J = 16.4 Hz, styryl –CH=C-), 7.35 (2H, d, J = 8.4 Hz, Ar–H), 7.45 (2H, d, J = 8.4 Hz, Ar–H), 7.50 (1H, d, J = 16.4 Hz, styryl –C=CH-), 7.63 (2H, d, J = 8.8 Hz, Ar–H), 7.83 (2H, d, J = 8.8 Hz, Ar–H), 8.22 (2H, d, J = 8.8 Hz, Ar–H), 8.29 (1H, s, Triazole-H). ^{13}C NMR (400 MHz, DMSO-d_6): δ = 52.02, 61.14, 115.11, 124.23, 124.83, 126.92, 128.63, 128.79, 129.27, 129.93, 132.96, 134.35, 135.01, 142.88, 144.49, 145.82, 158.56. +MS (ESI) m/z: 447.1 (447.9).

2.3. Bio-evaluation

2.3.1. Cytostatic assays

All tumor cell lines were acquired from the American Type Culture Collection (ATCC, Manassas, VA, USA), except for the DND-41 cell line, which was purchased from Deutsche Sammlung von Mikroorganismen und Zellkulturen (DSMZ Leibniz-Institut, Braunschweig, Germany). All cell lines were cultured as recommended by the suppliers. Media were purchased from GIBCO Life Technologies, USA, and supplemented with 10% fetal bovine serum (HyClone, GE Healthcare Life Sciences, USA). For real-time monitoring, adherent cell lines HCT-116, NCI–H460, and Capan-1 were seeded at a density between 500 and 1500 cells per well in 384-well clear-bottomed tissue culture plates (Greiner). After overnight incubation, cells were treated with the test compounds at seven different concentrations ranging from 100 to 6.4 × 10^{-3} μM. Suspension cell lines K-562, Z-138, and DND-41 were seeded at densities ranging from 2500 to 5000 cells per well in 384-well clear-bottomed tissue culture plates containing the test compounds at the same seven concentration points. The plates were incubated and monitored at 37 °C for 72 h in the IncuCyte® system (Essen BioScience Inc., Ann Arbor, MI, USA) for real-time imaging. Images were taken every 3 h, with one field imaged per well under 10× magnification. Cell growth was then quantified based on percent cellular confluence as analyzed by the IncuCyte® image analysis software and used to determine the IC_{50} values.

2.3.2. Methodology for in silico studies

The 3D structures of all compounds were prepared using Avogadro v1.2.0 [28] and their energies were minimized with the MMFF94s force field. The ADME properties, pharmacokinetic properties, and drug-likenesses of the compounds were then investigated with the SwissADME webserver [22, 23]. Finally, docking simulations of all compounds were performed with the crystal structure of a tubulin heterodimer (PDB ID: 1TUB) [24]. All ligands and the target were

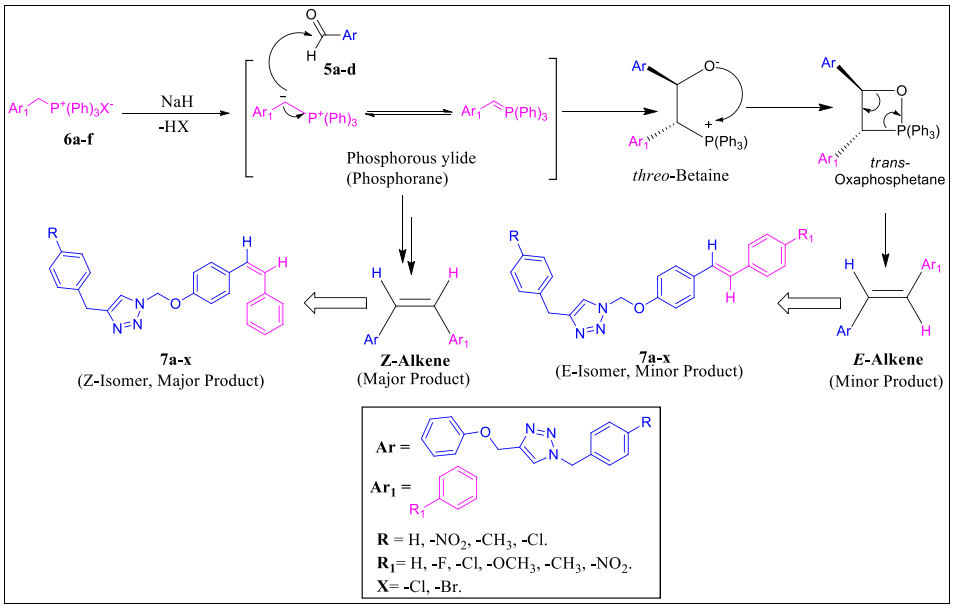

Figure 2. Mechanism of synthesis for 7a-x.

prepared using PyRx software [29] and the docking experiments were subsequently carried out using AutoDock Vina software [30] with the Lamarckian genetic algorithm (LGA) [31, 32]. The visualizations of docking simulation results were conducted using the Discovery studio [33].

3. Results and discussion

3.1. Chemistry

Series of (*E*)-1-benzyl-4-((4-styrylphenoxy)methyl)-1*H*-1,2,3-triazoles (**7a-x**) were obtained by Wittig reaction (Figure 2) [34] between the

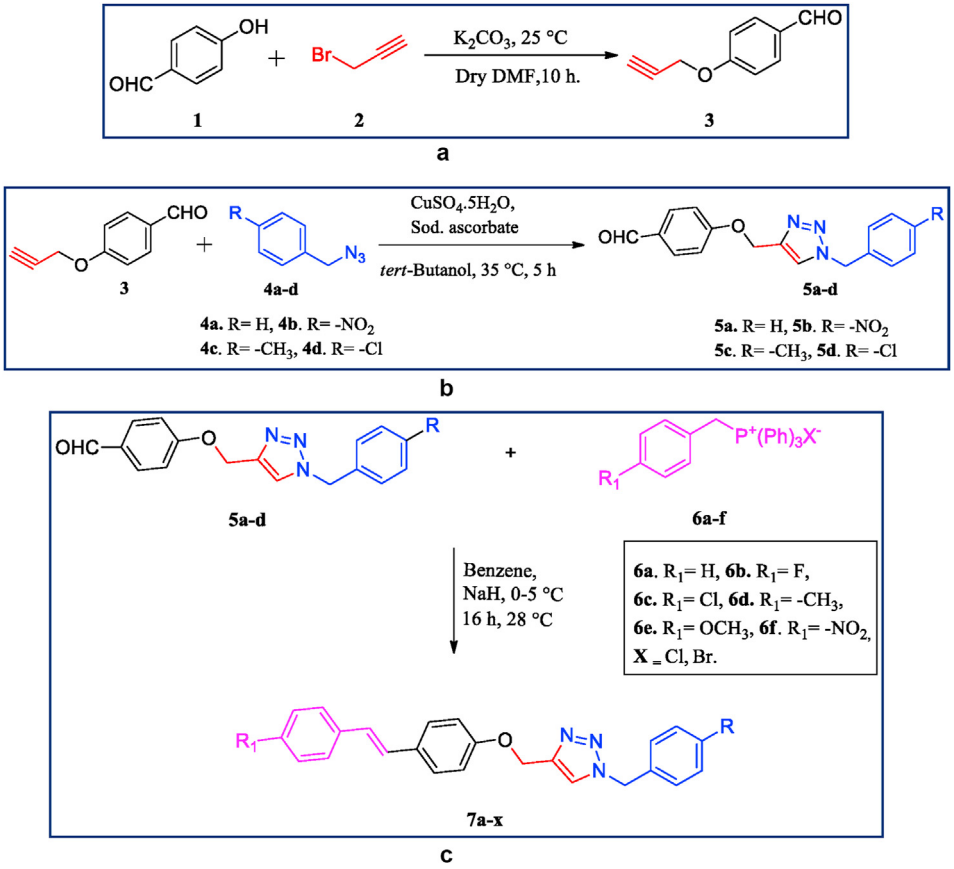

Scheme 1. a. Synthesis of 4-(prop-2-yn-1-yloxy)benzaldehyde (3). b. Synthesis of 4-((1-benzyl-1*H*-1,2,3-triazol-4-yl)methoxy)benzaldehydes (5a-d). c. Synthesis of *(E)*-1-benzyl-4-((4-styrylphenoxy)methyl)-1*H*-1,2,3-triazoles (7a-x).

Table 1. Synthesized stilbene linked 1,2,3-triazole analogues (**7a-x**).

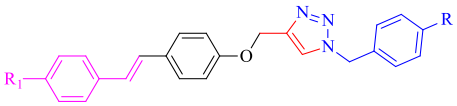

Compound	R_1	R	Molecular weight	Molecular formula	Melting point (°C)	Yield (%)	Purity (%)
7a	H	H	367.44	$C_{24}H_{21}N_3O$	202–204	35	100
7b	F	H	385.43	$C_{24}H_{20}FN_3O$	180–182	45	100
7c	Cl	H	401.89	$C_{24}H_{20}ClN_3O$	229–230	39	100
7d	CH_3	H	381.47	$C_{25}H_{23}N_3O$	102–104	28	100
7e	OCH_3	H	397.47	$C_{24}H_{23}N_3O_2$	190–192	39	100
7f	NO_2	H	412.44	$C_{24}H_{20}N_4O_3$	176–177	36	100
7g	H	NO_2	412.44	$C_{24}H_{20}N_4O_3$	145–147	45	100
7h	F	NO_2	430.43	$C_{24}H_{19}FN_4O_3$	182–184	32	100
7i	Cl	NO_2	446.89	$C_{24}H_{19}ClN_4O_3$	190–192	28	100
7j	CH_3	NO_2	426.47	$C_{25}H_{22}N_4O_3$	208–211	42	100
7k	OCH_3	NO_2	442.47	$C_{25}H_{22}N_4O_4$	207–209	28	100
7l	NO_2	NO_2	457.44	$C_{24}H_{19}N_5O_5$	207–208	33	100
7m	H	CH_3	381.47	$C_{25}H_{23}N_3O$	174–176	32	100
7n	F	CH_3	399.46	$C_{25}H_{22}FN_3O$	204–206	42	100
7o	Cl	CH_3	415.91	$C_{25}H_{22}ClN_3O$	187–190	42	100
7p	CH_3	CH_3	395.50	$C_{26}H_{25}N_3O$	200–202	35	100
7q	OCH_3	CH_3	411.50	$C_{26}H_{25}N_3O_2$	166–168	42	100
7r	NO_2	CH_3	426.47	$C_{25}H_{22}N_4O_3$	148–150	34	91
7s	H	Cl	401.89	$C_{24}H_{20}ClN_3O$	170–171	42	88
7t	F	Cl	419.88	$C_{24}H_{19}ClFN_3O$	170–172	36	100
7u	Cl	Cl	436.33	$C_{24}H_{19}Cl_2N_3O$	128–130	35	100
7v	CH_3	Cl	415.91	$C_{24}H_{22}ClN_3O$	165–166	42	100
7w	OCH_3	Cl	431.91	$C_{25}H_{22}ClN_3O_2$	192–194	35	100
7x	NO_2	Cl	446.89	$C_{24}H_{19}ClN_4O_3$	174–176	39	100

respective 4-((1-benzyl-1*H*-1,2,3-triazol-4-yl)methoxy) benzaldehydes (**5a-d**) and benzyltriphenylphosphonium halides (chlorides and bromide) (**6a-f**). Compounds **5a-d** were obtained *via* copper (Cu)-catalyzed regioselective 1,3-dipolar cycloaddition of 4-(prop-2-ynyloxy)benzaldehyde (**3**) with benzyl azides (**4a-d**), while the reaction between 4-hydroxybenzaldehyde (**1**) and propargyl bromide (**2**) led to compound **3**. Schemes 1a-c represent the synthetic routes and Table 1 contains the structures of **7a-x**. Structural confirmation was performed with Fourier transform infrared (FTIR), nuclear magnetic resonance (NMR) spectroscopy and mass spectrometry.

The FTIR spectra of compounds **7a-x** showed stretching peaks in the ranges of 3010–3101 (-CH, ar.), 2734–2964 (-CH, ali.), 1513–1634 (>C=N-), 1507–1516 (>C=C<), and 1176–1266 (-O-) cm^{-1} for the groups given in parentheses. Methylene ($–CH_2–$) bending peaks appeared in the range of 1427–1492 cm^{-1}. Compounds **7d**, **7e**, **7j**, **7k**, **7m-r**, **7v**, and **7w** showed methyl ($-CH_3$) bending peaks in the range of 1336–1395 cm^{-1}, while the nitro ($-NO_2$) stretching in **7f-l**, **7r**, and **7x** appeared between 1514 and 1592 cm^{-1}.

^{1}H NMR spectra showed singlet triazole ring protons in the range of 8.20–8.38 δ ppm. The aromatic protons appeared between 6.93 and 8.25 δ ppm while two doublet peaks appeared in the range of 7.06–7.50 δ ppm for ***E***-CH=CH of styryl moiety [35, 36]. Peaks at 5.40–5.80 and 5.13–5.20 δ ppm represent -N–CH_2– and –OCH_2-, respectively. The –CH_3 protons of **7d**, **7j**, **7m-r**, and **7v** appeared between 2.27 and 2.29 δ ppm along with -O-CH_3 protons of **7e**, **7k**, **7q**, and **7w** at 3.76 δ ppm. The nature of the carbon in **7a-x** was ascertained by the respective ^{13}C NMR spectral data. Absence of the –C≡CH proton of **3** at 1.56 δ ppm and presence of additional -N–CH_2– protons at 5.52 δ ppm along with singlet triazole-H at 7.59 δ ppm in **5a** confirmed the reaction between **3** and **4a**. Table 1 contains details of compounds **7a-x** such as molecular weight, molecular formula, yield, percentage purity, and physical constant.

3.2. Biological study

In vitro cellular cytotoxicity evaluations of derivatives **7a-x** were performed using six different human cancer cell lines (Capan-1, HCT-116, NCI–H460, DND-41, K-562, and Z-138) in 384-well micro-titer plates [37]. The tubulin inhibitor docetaxel [38] and the pan-kinase inhibitor staurosporine (STS) [39] were used as reference compounds and dimethyl sulfoxide (DMSO) as a solvent. The cytotoxicity data summarized in Table 2 represent 50% inhibitory concentrations (IC_{50}).

Irrespective of the substituents on the aromatic ring system, compounds **7a-x** were found to be poorly cytotoxic towards acute lymphoma (**DND-41**), chronic myeloid leukemia (**K-562**), Non Hodgin lymphoma (**Z-138**) and moderate cytotoxic against pancreatic adeno carcinoma (**Capan-1**), colorectal carcinoma (**HCT-116**), lung carcinoma (**NCI–H460**). In general, among the tested derivatives, **7a** and **7c** showed some cytotoxic chronic myeloid leukemia (**K-562**) cells. Most of the compounds displayed some sort of cytotoxic activity 31–96 μM against pancreatic adeno carcinoma (**Capan-1**) cells except compounds **7d**, **7g**, **7v** and **7x**. For colorectal carcinoma cells (**HCT-116**), the cytotoxic activity exhibited by many compounds of the series ranging from 12-87 μM. Among this series, **7e**, **7h** and **7k** were the most potent with IC50 at 12–13 μM, many compounds such as **7a**, **7g**, **7i**, **7q** and **7r** were cytotoxic in the range of 20–30 μM. For lung carcinoma (**NCI–H460**) cells, 12–16 μM cytotoxicity activity showed by compounds **7h**, **7r** and **7w,** whereas remaining compounds exhibited the activity ˃30 μM. In case of acute lymphoblastc leukemia (**DND-41**), very limited compounds namely **7a**, **7g** and **7o** displayed some cytotoxic activity 60–80 μM, remaining all compounds did not display any cytotoxic activity. Even for the chronic myeloid leukemia (**K-562**) cells also not showed any activity by the synthesized compounds except **7a** and **7c** with 40 and 19 μM. Similarly, for Non Hodgin lymphoma (**Z-138**), one compound that is **7d** showed some cytotoxic activity with IC50 60μM, and remaining compounds in

Table 2. *In-vitro* cytotoxicity data of synthesized stilbene linked 1,2,3-triazoles **7a-x** (μM).

Compound	Capan-1	HCT-116	NCI–H460	DND-41	K-562	Z-138
	Pancreatic adeno-carcinoma	Colorectal carcinoma	Lung carcinoma	Acute lymphoblastic leukemia	Chronic myeloid leukemia	Non-Hodgkin lymphoma
7a	46.7	29.1	34.3	61.4	39.9	>100
7b	30.7	46.7	31.7	>100	>100	>100
7c	96.4	36.1	>100	>100	19.3	>100
7d	>100	>100	81.7	>100	>100	60.3
7e	55.3	13.5	35.1	>100	>100	>100
7f	45.3	62.4	40.7	>100	>100	>100
7g	>100	26.1	78.5	82.1	>100	>100
7h	40.2	12.2	11.6	>100	>100	>100
7i	62.3	21.3	31.3	>100	>100	>100
7j	62.3	>100	98.3	>100	>100	>100
7k	50.2	12.6	95.4	>100	>100	>100
7l	70.3	76.7	44.3	>100	>100	>100
7m	45.9	>100	41.7	>100	>100	>100
7n	73.4	>100	>100	>100	>100	>100
7o	51.8	>100	47.3	81.2	>100	>100
7p	52.4	87.4	60.8	>100	>100	>100
7q	34.6	30.5	37.1	>100	>100	>100
7r	39.5	21.3	16.2	>100	>100	>100
7s	80.6	33	61.1	>100	>100	>100
7t	67.3	71.5	91.9	>100	>100	>100
7u	41.3	36.5	33.8	>100	>100	>100
7v	>100	57.3	>100	>100	>100	>100
7w	48.9	36	12.4	>100	>100	>100
7x	>100	55.8	72.5	>100	>100	>100
Docetaxel	0.0063	0.0008	0.0001	0.0019	0.0034	0.0019
STS	0.0046	0.0003	0.0032	0.0064	0.0298	0.0003

the series failed to display activity. By looking at the cytotoxicity results from Table 2, the most of the compounds tested in the series were cytotoxic only against carcinoma cells but not active or cytotoxic to leukemia and lymphoma but none of the tested compounds was not potent as compared to both the drug standards. The compounds shown in Figure 3 are the most active members of the series.

3.3. *In silico analyses*

Table 3 shows the physicochemical properties, ADME parameters, and violations of drug-likeness rules of the synthesized compounds. Calculated physicochemical and lipophilicity parameters are used by various filters to evaluate the drug-likeness of synthesized compounds and, in this paper, we evaluated the drug-likeness properties of the compounds with the most significant filtering approaches in the literature. The filters used here and their rules are as follows:

- Lipinski (Pfizer) filter [40]: MW $\leq$ 500; MLOGP $\leq$4.15; HBA $\leq$10; HBD $\leq$5
- Ghose filter [41]: 160 $\leq$ MW $\leq$ 480; -0.4 $\leq$ WLOGP $\leq$5.6; 40 $\leq$ MR $\leq$ 130; 20 $\leq$ atoms $\leq$70
- Veber (GSK) filter [42]: RB $\leq$ 10; TPSA $\leq$140
- Egan (Pharmacia) filter [43]: WLOGP $\leq$5.88; TPSA $\leq$131.6
- Muegge (Bayer) filter [44]: 200 $\leq$ MW $\leq$ 600, -2 $\leq$ XLOGP $\leq$5; TPSA $\leq$157; HBA $\leq$10; HBD $\leq$5; RB $\leq$ 15; number of rings $\leq$7; number of carbons >4; number of heteroatoms >1.

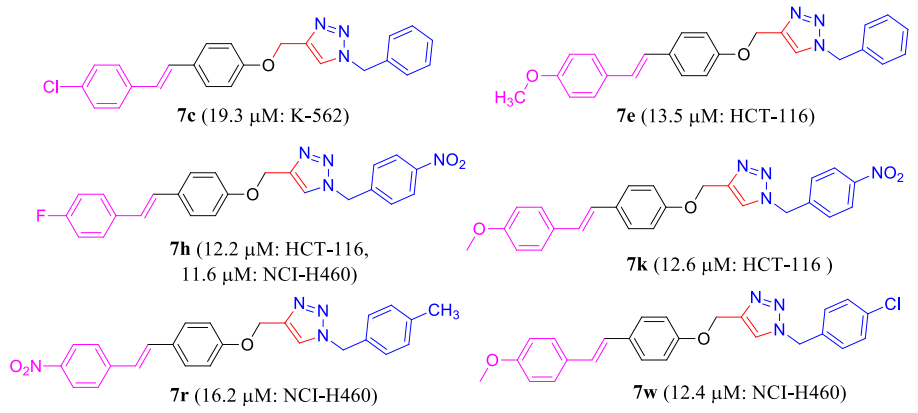

Figure 3. Biologically active stilbene linked 1,2,3-triazole derivatives.

Table 3. Physicochemical and pharmacokinetic properties of stilbene linked 1,2,3-triazoles.

Comp.	Binding affinity	Physicochemical Properties							Lipophilicity						Drug-likeness					Water Solubility		Pharmacokinetics	
		MW (g/mol)	Fsp^3	RB	HBA	HBD	MR	tPSA	ilogP	XlogP3	WlogP	MlogP	SILICOS-IT	Consensus logP	Lipinski	Ghose	Veber	Egan	Muegge	ESOL	Class	Log K_p (cm/s)	F
7a	-10.3	367.44	0.08	7	3	0	112.12	39.94	3.83	5.05	4.71	4.01	4.86	4.49	0	0	0	0	1	-5.45	Moderately	-4.96	0.55
7b	-9.9	385.43	0.08	7	4	0	112.08	39.94	3.84	5.15	5.27	4.38	5.27	4.78	1	0	0	0	1	-5.60	Moderately	-4.99	0.55
7c	-10.6	401.89	0.08	7	3	0	117.13	39.94	4.18	5.68	5.36	4.49	5.49	5.04	1	0	0	0	1	-6.04	Poorly	-4.72	0.55
7d	-10.4	381.47	0.12	7	3	0	117.09	39.94	4.03	5.42	5.01	4.22	5.38	4.81	1	0	0	0	1	-5.74	Moderately	-4.78	0.55
7e	-10.3	397.47	0.12	8	4	0	118.61	49.17	4.23	5.03	4.71	3.66	4.91	4.51	0	0	0	0	1	-5.51	Moderately	-5.15	0.55
7f	-10.1	412.44	0.08	8	5	0	120.94	85.76	3.50	4.88	4.61	3.86	2.68	3.91	0	0	0	0	0	-5.49	Moderately	-5.35	0.55
7g	-9.7	412.44	0.08	8	5	0	120.94	85.76	3.53	4.88	4.61	3.86	2.68	3.91	0	0	0	0	0	-5.49	Moderately	-5.35	0.55
7h	-11.2	430.43	0.08	8	6	0	120.90	85.76	3.55	4.98	5.17	4.24	3.10	4.21	1	0	0	0	0	-5.65	Moderately	-5.39	0.55
7i	-10.2	446.89	0.08	8	5	0	125.95	85.76	3.74	5.51	5.27	4.34	3.32	4.44	1	0	0	0	1	-6.09	Poorly	-5.11	0.55
7j	-10.5	426.47	0.12	8	5	0	125.91	85.76	3.84	5.25	4.92	3.26	3.21	4.10	0	0	0	0	1	-5.80	Moderately	-5.17	0.55
7k	-10.3	442.47	0.12	9	6	0	127.43	94.99	3.72	4.85	4.62	2.74	2.75	3.74	0	0	0	0	0	-5.56	Moderately	-5.56	0.55
7l	-10.1	457.44	0.08	9	7	0	129.76	131.58	3.29	4.71	4.52	3.01	0.53	3.21	0	0	0	0	0	-5.55	Moderately	-5.75	0.55
7m	-9.6	381.47	0.12	7	3	0	117.09	39.94	4.09	5.42	5.01	4.22	5.38	4.83	1	0	0	0	1	-5.74	Moderately	-4.78	0.55
7n	-10.2	399.49	0.12	7	4	0	117.04	39.94	4.28	5.52	5.57	4.59	5.80	5.15	1	0	0	0	1	-5.90	Moderately	-4.82	0.55
7o	-10.2	415.91	0.12	7	3	0	122.10	39.94	4.42	6.05	5.67	4.69	6.02	5.37	1	1	0	0	1	-6.34	Poorly	-4.54	0.55
7p	-10.5	395.50	0.15	7	3	0	122.05	39.94	4.27	5.78	5.32	4.42	5.91	5.14	1	0	0	0	1	-6.04	Poorly	-4.61	0.55
7q	-10.5	411.50	0.15	8	4	0	123.58	49.17	4.54	5.39	5.02	3.86	5.44	4.85	0	0	0	0	1	-5.81	Moderately	-4.98	0.55
7r	-10.9	426.47	0.12	8	5	0	125.91	85.76	3.87	5.25	4.92	3.26	3.21	4.10	0	0	0	0	1	-5.80	Moderately	-5.17	0.55
7s	-9.3	401.89	0.08	7	3	0	117.13	39.94	4.14	5.68	5.36	4.49	5.49	5.03	1	0	0	0	1	-6.04	Poorly	-4.72	0.55
7t	-9.7	419.88	0.08	7	4	0	117.09	39.94	4.21	5.78	5.92	4.86	5.91	5.33	1	1	0	1	1	-6.19	Poorly	-4.76	0.55
7u	-10.0	436.33	0.08	7	3	0	122.14	39.94	4.34	6.31	6.01	4.96	6.13	5.55	1	1	0	1	1	-6.63	Poorly	-4.48	0.55
7v	-10.2	415.91	0.12	7	3	0	122.10	39.94	4.27	6.05	5.67	4.69	6.02	5.34	1	1	0	0	1	-6.34	Poorly	-4.54	0.55
7w	-10.4	431.91	0.12	8	4	0	123.62	49.17	4.44	5.65	5.37	4.13	5.55	5.03	0	0	0	0	1	-6.10	Poorly	-4.92	0.55
7x	-10.5	446.89	0.08	8	5	0	125.95	85.76	3.73	5.51	5.27	4.34	3.32	4.43	1	0	0	0	1	-6.09	Poorly	-5.11	0.55
Docetaxel	-9.4	807.88	0.56	14	14	5	205.25	224.45	4.30	2.81	2.94	1.06	3.51	2.92	2	3	2	1	3	-5.85	Moderately	-9.23	0.17
STS	-10.8	466.53	0.32	2	4	2	139.39	69.45	3.19	3.24	3.39	2.60	3.02	3.09	0	1	0	0	1	-5.06	Moderately	-6.85	0.55

Molecular weight: MW, topological polar surface area: tPSA, Molar Refractivity: MR, fraction of sp^3 carbon atoms: Fsp^3, HBD: hydrogen bonds donor, HBA: hydrogen bond acceptor, RB: rotatable bonds, LogP values: indicator of Lipophilicity, ESOL: aqueous solubility parameter, Log K_p: skin permeation, F: Bioavailability Score.

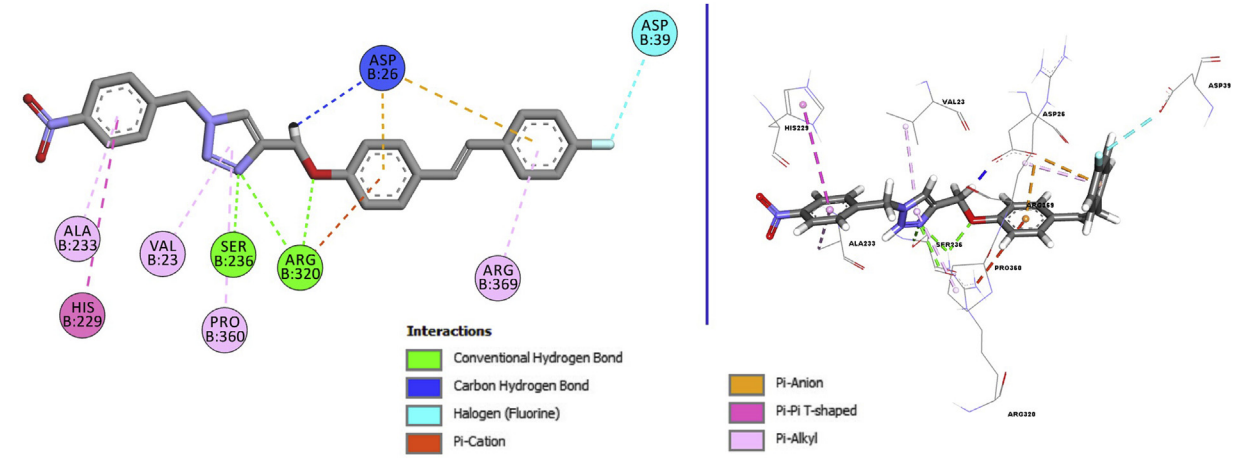

Figure 4. The 2D and 3D representations of interactions between compound **7h** and 1TUB receptor.

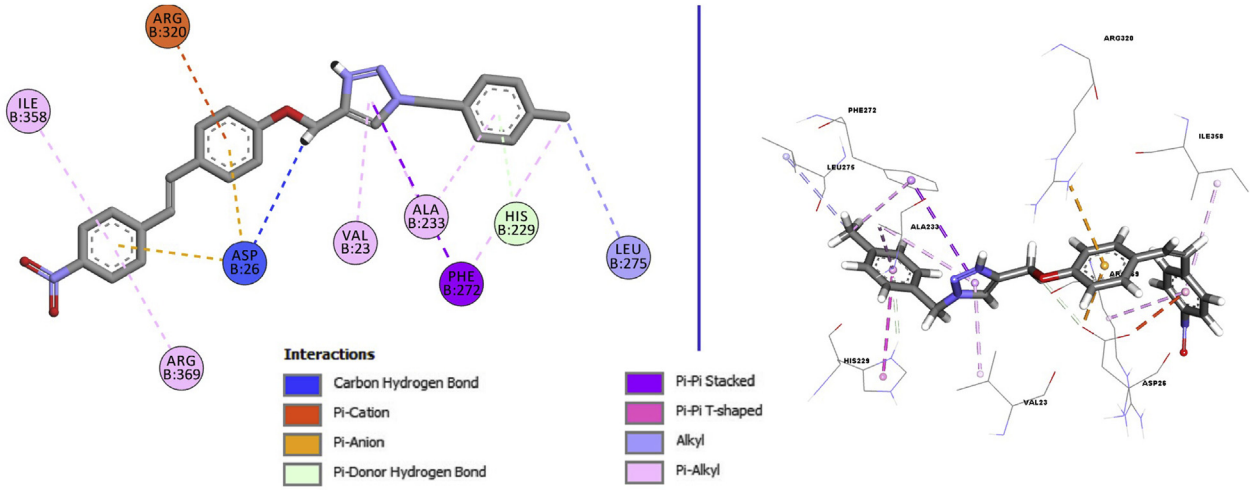

Figure 5. The 2D and 3D representations of interactions between compound **7r** and 1TUB receptor.

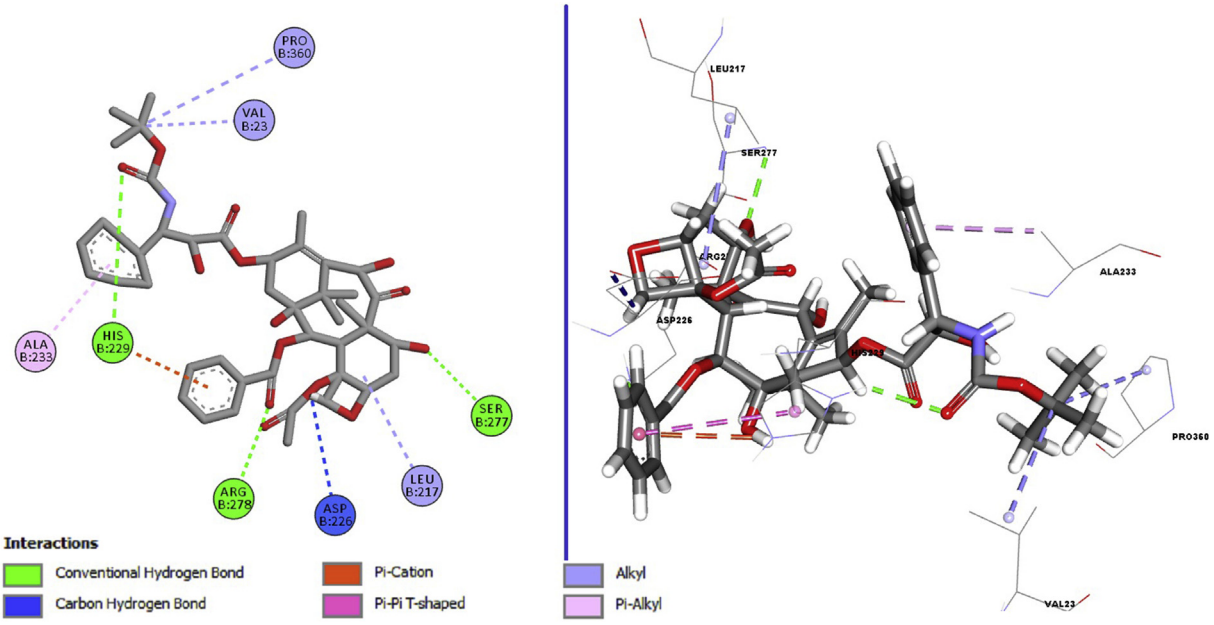

Figure 6. The 2D and 3D representations of interactions between docetaxel (co-ligand) and 1TUB receptor.

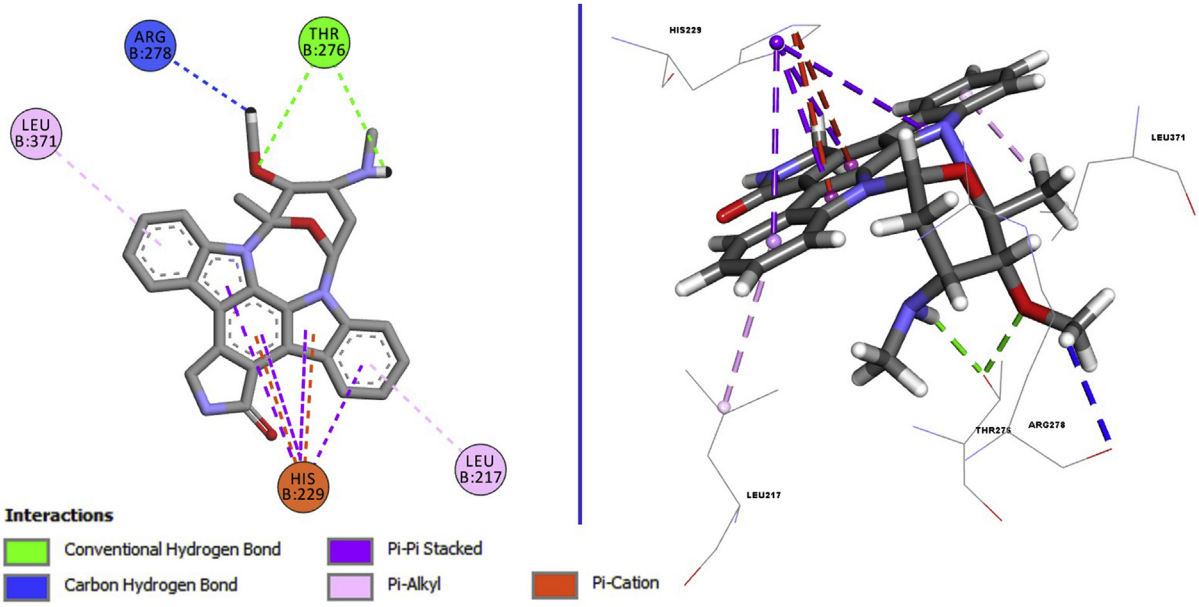

Figure 7. The 2D and 3D representations of interactions between STS and 1TUB receptor.

The filters generally assume that an orally active drug should not violate the above criteria more than once. When Table 3 is examined, it can be said that all newly synthesized compounds and the reference drug STS meet these criteria. However, the other reference drug, docetaxel, is observed to violate all filters more than once, except the Muegge filter.

Fsp^3 is another newly introduced parameter [45] to interpret the drug-likeness properties of molecules. According to Table 3, the Fsp^3 values of all compounds are lower than those of docetaxel and STS. Furthermore, we observed that the ESOL values of all synthesized compounds belonged to the moderately water-soluble class. Compounds **7c**, **7j**, **7o**, **7p**, **7s**, **7t**, **7u**, **7v**, **7w**, and **7x** have values greater than -6; thus, they are in the poorly soluble class. On the other hand, other newly synthesized compounds and reference drugs are in the moderately soluble class. Log K_p in the table is the skin permeation parameter suggested by Potts et al. [46], and a low negative log K_p value of a compound corresponds to higher absorption into human skin. Accordingly, all newly synthesized compounds have higher levels of skin absorption than the reference drugs. In the table, the bioavailability score (F) of the compounds signifies the probability that a compound will have oral bioavailability in rats [47]. The newly synthesized compounds and STS have higher F scores than docetaxel.

We also conducted molecular docking simulations to help elucidate the anticancer activities of the synthesized compounds. In the docking simulations, we utilized the crystal structure of the tubulin-docetaxel complex [24] (PDB ID: 1TUB) as the target. The binding affinity values obtained as a result of the docking studies are shown in Table 3. As is seen there, compounds **7h** and **7r**, which show good cytotoxicity *in vitro*, have the highest binding energy values. It was also observed that the reference drug STS had a higher binding affinity than the other reference drug, docetaxel, which is also the co-ligand of 1TUB. In this context, to identify the binding regions of **7h, 7r**, STS, and docetaxel, we display the two-dimensional (2D) interaction diagrams and 3D interactions between these compounds and 1TUB in Figures 4, 5, 6, and 7.

As seen in Figures 4, 5, 6, and 7, compound **7h** has a total of 4 hydrogen bond interactions, including 3 conventional hydrogen bonds (coHB) and 1 carbon hydrogen bond (caHB). Compound **7h** also has 3 electrostatic interactions (2 pi-anion (PA), 1 pi-cation (PC)), 5 hydrophobic interactions (1 pi-pi T-shaped (PT), 3 pi-alkyl (PAl)), and 1 halogen interaction. On the other hand, compound **7r** has 2 hydrogen bonds (1 coHB, 1 pi-donor hydrogen bond (pdHB)), 3 electrostatic interactions (1 PC, 2 PA), and 9 hydrophobic interactions (2 PT, 6 PAl, 1 Alkyl (Al)).

For reference compounds docetaxel and STS, it can be said that docetaxel has 3 hydrogen bonds (3 coHB, 1 caHB), 1 electrostatic interaction (1 PC), and 8 hydrophobic interactions (1 PT, 2 PAl, 5 Al), whereas STS has 2 hydrogen bonds (3 coHB, 1 caHB), 2 electrostatic interactions (1 PC), and 6 hydrophobic interactions (2 PAl, 4 pi-pi stacked (PSt)). In this case, the PSt interactions of STS may have caused STS to show higher affinity for 1TUB than docetaxel.

4. Conclusions

24 derivatives of resveratrol linked 1,2,3-triazole (**7a-x)** were synthesized, characterized by ^1H, ^{13}C NMR, Mass Spectrometry and FTIR. All the compounds tested for their cytotoxic study against three carcinoma, two leukemia and one lymphoma human cancer cell lines. Most of the compounds tested in the series were cytotoxic towards all three types of carcinoma cells but were not cytotoxic to leukemia and lymphoma. In the docking simulations, we docked all the compounds with protein 1TUB. Compounds **7h** and **7r**, which showed good cytotoxicity *in vitro*, have the highest binding energy values. We identified according to docking results that compound **7h** has four hydrogen bond, three electrostatic interactions, five hydrophobic interactions, and one halogen interaction while another compound **7r** has two hydrogen bonds, three electrostatic interactions, and nine hydrophobic interactions. Therefore, resveratrol linked 1,2,3-triazoles were more sensitive towards human carcinoma cell lines but least sensitive towards leukemia and lymphoma cell lines. Hence, further optimization is required to obtain an effective lead molecule against cancer.

Declarations

Author contribution statement

A. Das: Performed the experiments; Contributed reagents, materials, analysis tools or data.

D. Daelemans: Performed the experiments.

L. Persoons: Performed the experiments.

D. Schols: Analyzed and interpreted the data; Contributed reagents, materials, analysis tools or data; Wrote the paper.

S. S Karki: Conceived and designed the experiments; Analyzed and interpreted the data; Wrote the paper.

S. Kumar: Contributed reagents, materials, analysis tools or data; Wrote the paper.

H. Alici: Conceived and designed the experiments; Performed the experiments; Contributed reagents, materials, analysis tools or data.

H. Tahtaci: Analyzed and interpreted the data; Wrote the paper.

Funding statement

This work was supported by Federal funds from the Division of Microbiology and Infectious Diseases, National Institute of Allergy and Infectious Diseases, National Institutes of Health, Department of Health and Human Services, under Contract No. 75N93019D00005.

Data availability statement

Data will be made available on request.

Declaration of interests statement

The authors declare no conflict of interest.

Additional information

Supplementary content related to this article has been published online at https://doi.org/10.1016/j.heliyon.2020.e05893.

References

[1] V. Schirrmacher, From chemotherapy to biological therapy: a review of novel concepts to reduce the side effects of systemic cancer treatment, Int. J. Oncol. 54 (2019) 407–419.
[2] P. Simon, The importance of heterocyclic compounds in anti-cancer drug design, Drug Discov. World Summer (2017) 66–70.
[3] X.-L. Wang, K. Wan, C.-H. Zhou, Synthesis of novel sulfanilamide-derived 1,2,3-triazoles and their evaluation for antibacterial and antifungal activities, Eur. J. Med. Chem. 45 (2010) 4631–4639.
[4] Y.-W. He, C.-Z. Dong, J.-Y. Zhao, L.-L. Ma, Y.-H. Li, H.A. Aisa, 1,2,3-Triazole-containing derivatives of rupestonic acid: clickchemical synthesis and antiviral activities against influenza viruses, Eur. J. Med. Chem. 76 (2014) 245–255.
[5] D. Dheer, V. Singh, R. Shankar, Medicinal attributes of 1,2,3- triazoles: current developments, Bioorg. Chem. 71 (2017) 30–54.
[6] C.P. Kaushik, J. Sangwan, R. Luxmi, D. Kumar, D. Kumar, A. Das, A. Kumar, D. Singh, Design, synthesis, anticancer and antioxidant activities of amide linked 1,4-disubstituted 1,2,3- triazoles, J. Mol. Struct. 1226 (2021) 129255.
[7] S. Murugavel, C. Ravikumar, G. Jaabil, Ponnuswamy Alagusundaram, Synthesis, computational quantum chemical study, in silico ADMET and molecular docking analysis, in vitro biological evaluation of a novel sulfur heterocyclic thiophene derivative containing 1,2,3- triazole and pyridine moieties as a potential human topoisomerase IIα inhibiting anticancer agent, Comput. Biol. Chem. 79 (2019) 73–82.
[8] P. Yadav, K. Lal, A. Kumar, S.K. Guru, S. Jaglan, S. Bhushan, Green synthesis and anticancer potential of chalcone linked-1,2,3-triazoles, Eur. J. Med. Chem. 126 (2017) 944–953.
[9] J.H. Hart, Role of phytostilbenes in decay and disease resistance, Annu. Rev. Phytopathol. 19 (1991) 437–458.
[10] J. Burns, T. Yokota, H. Ashihara, M.E. Lean, A. Crozier, Plant foods and herbal sources of resveratrol, J. Agric. Food Chem. 50 (2002) 3337–3340.
[11] G.J. Soleas, E.P. Diamandis, D.M. Goldberg, Resveratrol: a molecule whose time has come? and gone? Clin. Biochem. 30 (1997) 91–113.
[12] H.B. Zhou, J.J. Chen, W.X. Wang, J.T. Cai, Q. Du, Anticancer activity of resveratrol on implanted human primary, World J. Gastroenterol. 11 (2005) 280–284.
[13] C.R. Pace-Asciak, S. Hahn, E.P. Diamandis, G. Soleas, D.M. Goldberg, The red wine phenolics trans-resveratrol and quercetin block human platelet aggregation and eicosanoid synthesis implications for protection against coronary heart disease, Clin. Chim. Acta 235 (1995) 207–219.
[14] J. Griggs, J.C. Metcalfe, R. Hesketh, Targeting tumour vasculature: the development of combretastatin A4, Lancet Oncol. 2 (2001) 82–87.
[15] M. Mokni, S. Elkahoui, F. Limam, M. Amri, E. Aouani, Effect of resveratrol on antioxidant enzyme activities in the brain of healthy rat, Neurochem. Res. 32 (2007) 981–987.
[16] D. Simoni, M. Roberti, F.P. Invidiata, E. Aiello, S. Aiello, P. Marchetti, R. Baruchello, M. Eleopra, A.D. Cristina, S. Grimaudo, N. Gebbia, L. Crosta, F. Dieli, M. Tolomeo, Stilbene- based anticancer agents: resveratrol analogues active toward HL 60 leukemic cells with a non-specific phase mechanism, Bioorg. Med. Chem. Lett 16 (2006) 3245–3248.
[17] A. Cirla, J. Mann, Combretastatins: from natural products to drug discovery, Nat. Prod. Rep. 20 (2003) 558–564.
[18] R. Cassano, F. De Amicis, C. Servidio, F. Curcio, S. Trombino, Preparation, characterization and in vitro evaluation of resveratrol-loaded nanospheres potentially useful for human breast carcinoma, J. Drug Deliv. Sci. Technol. 57 (2020) 101748.
[19] K.-Y. Kang, J.-K. Shin, S.-M. Lee, Pterostilbene protects against acetaminophen-induced liver injury by restoring impaired autophagic flux, Food Chem. Toxicol. 123 (2019) 536–545.
[20] M. Rostami, M. Ghorbani, M.A. Mohammadi, M. Delavar, M. Tabibiazar, S. Ramezani, Development of resveratrol loaded chitosan-gellan nanofiber as a novel gastrointestinal delivery system, Int. J. Biol. Macromol. 135 (2019) 698–705.
[21] X. Zheng, L.Y. Yu, X. Yao, B. Lv, Z.H. Yang, Q.T. Zheng, H.Y. Duan, C. Song, H.L. Xie, Synthesis and anti-cancer activities of resveratrol derivatives, Open J. Med. Chem. 6 (2016) 51–57.
[22] A. Daina, O. Michielin, V. Zoete, SwissADME: a free web tool to evaluate pharmacokinetics, drug-likeness and medicinal chemistry friendliness of small molecules, Sci. Rep. 7 (2017) 42717.
[23] A. Daina, O. Michielin, V. Zoete, iLOGP: a simple, robust, and efficient description of n-octanol/water partition coefficient for drug design using the GB/SA approach, J. Chem. Inf. Model. 54 (2014) 3284–3301.
[24] E. Nogales, S.G. Wolf, K.H. Downing, Erratum: structure of the αβ tubulin dimer by electron crystallography, Nature 393 (1998) 191, 191.
[25] L. Hong, W. Lin, F. Zhang, R. Liua, X. Zhou, Ln[N(SiMe3)2]3-catalyzed cycloaddition of terminal alkynes to azides leading to 1,5-disubstituted 1,2,3-triazoles: new mechanistic features, Chem. Commun. 49 (2013) 5589–5591.
[26] K. Lal, P. Yadav, A. Kumar, Synthesis, characterization and antimicrobial activity of 4-((1-benzyl/phenyl-1*H*-1,2,3-triazol-4-yl)methoxy)benzaldehyde analogues, Med. Chem. Res. 25 (2016) 644–652.
[27] S.S. Karki, S.R. Bhutle, G.S. Pedgaonkar, P.K. Zubaidha, R.M. Shaikh, C.G. Rajput, G.S. Shendarkar, Synthesis and biological evaluation of some stilbene-based analogues, Med. Chem. Res. 20 (2011) 1158–1163.
[28] M.D. Hanwell, D.E. Curtis, D.C. Lonie, T. Vandermeersch, E. Zurek, G.R. Hutchison, Avogadro: an advanced semantic chemical editor, visualization, and analysis platform, J. Cheminf. 4 (2012) 17.
[29] S. Dallakyan, A.J. Olson, Small-molecule Library Screening by Docking with PyRx, Chemical Biology, Springer, 2015, pp. 243–250.
[30] O. Trott, A.J. Olson, AutoDock Vina, Improving the speed and accuracy of docking with a new scoring function, efficient optimization, and multithreading, J. Comput. Chem. 31 (2010) 455–461.
[31] F.J. Solis, R.J.-B. Wets, Minimization by random search techniques, Math. Oper. Res. 6 (1981) 19–30.
[32] R. Huey, G.M. Morris, A.J. Olson, D.S. Goodsell, A semiempirical free energy force field with charge-based desolvation, J. Comput. Chem. 28 (2007) 1145–1152.
[33] D.S. Biovia, Discovery Studio Modeling Environment, Dassault Systèmes, San Diego, 2017.
[34] B.E. Maryanoff, A.B. Reitz, M.S. Mutter, R.R. Whittle, R. Olofson, Stereochemistry and mechanism of the Wittig reaction. Diasteromeric reaction intermediates and analysis of the reaction course, J. Am. Chem. Soc. 108 (1986) 7664–7678.
[35] V. Srivastava, H. Lee, Synthesis and bio-evaluation of novel quinolino-stilbene derivatives as potential anticancer agents, Bioorg. Med. Chem. 23 (2015) 7629–7640.
[36] Y.-C. Duan, Y.-Y. Guan, X.-Y. Zhai, L.-N. Ding, W.-P. Qin, D.-D. Shen, X.-Q. Liu, X.-D. Sun, Y.-C. Zheng, H.-M. Liu, Discovery of resveratrol derivatives as novel LSD1 inhibitors: design, synthesis and their biological evaluation, Eur. J. Med. Chem. 126 (2017) 246–258.
[37] K. Pavić, I. Perković, P. Gilja, F. Kozlina, K. Ester, M. Kralj, D. Schols, D. Hadjipavlou-Litina, E. Pontiki, B. Zorc, Design, synthesis and biological evaluation of novel primaquine-cinnamic acid conjugates of the amide and acylsemicarbazide type, Molecules 21 (2016) 1629.
[38] A. Montero, F. Fossella, G. Hortobagyi, V. Valero, Docetaxel for treatment of solid tumours: a systematic review of clinical data, Lancet Oncol. 6 (2005) 229–239.
[39] A. Gescher, Analogs of staurosporine: potential anticancer drugs? Gen. Pharmacol. 31 (1998) 721–728.
[40] C.A. Lipinski, F. Lombardo, B.W. Dominy, P.J. Feeney, Experimental and computational approaches to estimate solubility and permeability in drug discovery and development settings, Adv. Drug Deliv. Rev. 23 (1997) 3–25.
[41] A.K. Ghose, V.N. Viswanadhan, J.J. Wendoloski, A knowledge-based approach in designing combinatorial or medicinal chemistry libraries for drug discovery. 1. A qualitative and quantitative characterization of known drug databases, J. Comb. Chem. 1 (1999) 55–68.
[42] D.F. Veber, S.R. Johnson, H.-Y. Cheng, B.R. Smith, K.W. Ward, K.D. Kopple, Molecular properties that influence the oral bioavailability of drug candidates, J. Med. Chem. 45 (2002) 2615–2623.
[43] W.J. Egan, K.M. Merz, J.J. Baldwin, Prediction of drug absorption using multivariate statistics, J. Med. Chem. 43 (2000) 3867–3877.
[44] I. Muegge, S.L. Heald, D. Brittelli, Simple selection criteria for drug-like chemical matter, J. Med. Chem. 44 (2001) 1841–1846.
[45] F. Lovering, J. Bikker, C. Humblet, Escape from flatland: increasing saturation as an approach to improving clinical success, J. Med. Chem. 52 (2009) 6752–6756.
[46] R.O. Potts, R.H. Guy, Predicting skin permeability, Pharm. Res. (N. Y.) 9 (1992) 663–669.
[47] Y.C. Martin, A bioavailability score, J. Med. Chem. 48 (2005) 3164–3170.